OBSERVATIONS ON THE VIBRATIONS OF PAPER WEBS

by

A. Raman[1], K.-D. Wolf[2], and P. Hagedorn[2]
[1]Purdue University
USA
[2]Darmstadt University of Technology
GERMANY

ABSTRACT

Frequency clustering and edge vibration localization of thin, wide, high-speed translating webs are investigated using a linear, translating, tensioned Kirchhoff plate model with very small but finite bending stiffness to tension ratio. Non-uniform tensioning, and vibration coupling of the web with a incompressible potential flow are included in the model. Such webs are commonly found in paper, plastic, polymer sheet and metal foil processing, in gravure and offset web printing machines, and in magnetic and optical tapes. The presence of frequency clusters, its impact on free edge vibration localization, and its dependence on transport speed, and non-uniformity of tension are analyzed using a Galerkin discretization of the equations of motion. Experiments are performed on an acoustically excited, stationary, taut paper web. The experimental results demonstrate clearly the presence of frequency clustering and its dynamic effects. The results are expected to have significant implications for the further studies on the modal analysis and nonlinear mechanics of high-speed web systems.

NOMENCLATURE

a	Length of web span	N_{xy}	In-plane membrane shear force/length
b	Width of web	N_{yy}	Membrane normal force/length along Y
c	Web transport speed	N_0	Width averaged tension per unit length
D	Web bending stiffness, $D = Eh^3/12(1-\mu)$	p	Aerodynamic pressure difference on the web
E	Young's modulus of the web material	u	Eulerian description of transverse web deflection
h	Web thickness, m		
N_{xx}	Membrane normal force/length along X		

β	Tension non-uniformity parameter	ρ_{air}	Air density
ε	Bending stiffness to tension ratio, $\varepsilon = D/a^2 N_0$	ω	Web natural frequency
ϕ	Aerodynamic potential	ψ_{mn}	Basis function for discretization
κ	Web aspect ratio	Ψ_{mn}	Two-dimensional Fourier transform of ψ_{mn}
λ	System eigenvalue	Λ	Web density parameter, $\Lambda = a\rho_{air}/\rho$
μ	Web Poisson's ratio	∇^4	Biharmonic operator
ρ	Web mass per unit area		

INTRODUCTION

Paper, textiles, sheet metals, wide tapes, and plastics are usually processed as thin webs. These webs are tensioned in one direction and transported, often at high speeds, over rollers and guides. Transverse vibration and instability lead to diminished product quality and to increased web breakage. Prediction and suppression of undesirable web vibrations is important for the development of high-speed reduced-breakage webs.

Paper or textile webs have been modeled as isotropic membranes, orthotropic membranes or networks (Steigmann and Pipkin (1991)), and plates with small but finite bending stiffness. A large body of the literature deals with the wrinkling, or local buckling of webs under different boundary tractions. Steigmann and Pipkin (1991) use a relaxed energy density technique to predict wrinkled shapes of taut and partially slack, nonlinearly elastic networks. Lin and Mote (1996) predicted the wrinkled shapes in the presence of non-uniform boundary conditions using a linear plate theory with small stiffness-to-tension ratio. Mockensturm and Mote (1999) used a nonlinearly elastic shell model to predict the onset and buckled shapes under the influence of roller misalignment. Another body of work focuses on the equilibrium displacement of webs in the presence of surface or boundary traction or body forces. Amongst these, Steigmann and Pipkin (1991) deal with universal deformations of networks. Lin and Mote (1995) use a Von-Kármán plate theory with small stiffness-to-tension ratio to predict the deformation of stationary and traveling webs under transverse traction. However, the focus of the present paper is on the oscillations of a taut web about a flat equilibrium state, before the onset of wrinkling.

Several authors have investigated the vibrations of webs. Mockensturm (1999) in recent work considered the oscillations of webs that are twisted through roller misalignments. While this work predicts the natural frequencies of webs about a nonlinearly elastic equilibrium, it is focused towards predicting the onset of buckling and critical speed. The behavior of the oscillations at vanishing stiffness-to-tension ratio was also not analyzed in detail. Wang and Steigmann (1997) considered the linear oscillations of nonlinearly elastic nets about their nonlinear equilibrium under the influence of boundary traction. However in the case of webs that are tensioned only in one direction (partially slack in Steigmann's terminology), the equations of linear oscillations lose ellipticity. Transverse linear vibrations of partially webs tensioned only in one direction clearly require the introduction of bending stiffness, however small. In this regard Ulsoy and Mote (1982) studied the transverse vibrations of a uniaxially tensioned, flat, translating Kirchhoff plate. They demonstrated the effect of transport speed, in-plane membrane stresses, and damping on the plate frequencies. However, their model was motivated by applications to wide bandsaw vibrations, where the ratio of bending stiffness to applied tension is $O(1)$.

The present work re-examines the behavior of the linear transverse vibrations of isotropic, linearly elastic, stationary and translating webs along the lines of Ulsoy and Mote (1982), but focuses on the unique behavior of the web in the limit of vanishing stiffness-to-tension ratio, and in the presence of non-uniform tension and aerodynamic coupling. This limiting case is of particular importance in the processing of thin webs like those encountered in paper, textile, plastic and thin metallic webs. For instance, in a typical paper web of thickness $0.08mm$, areal mass density $90\,gm/m^2$ stretched over a span of $1m$ and under a tension of $60\,N/m$, the ratio of bending stiffness to tension times the square of the length of the span, $\varepsilon = O(10^{-7})$. For an aluminum web of similar proportions, $\varepsilon = O(10^{-4})$. Of particular interest, therefore, is the transition of the dispersive wave behavior in the limit of vanishing stiffness-to-tension ratio.

MODELING AND DISCRETIZATION OF THE TRAVELING WEB

Consider a thin, linearly elastic web stretched flat across rollers, tensioned in the X direction and translating along the X axis with constant velocity c as shown in the figure 1. The web is modeled as an isotropic, translating, Kirchhoff plate with a small ratio of bending stiffness to tension. The web is assumed to be simply supported at the upstream and downstream edges, $x = 0, a$, respectively. It has been shown previously Turnbull *et al.* (1995) that simply supported boundary conditions are a suitably accurate boundary condition for predicting the linear vibrations of webs stretched over finite radius rollers.

General membrane stress distributions are also modeled. These "residual" stresses in webs can arise from various sources: non-uniform distribution of stress upstream or downstream from the span; from roller misalignments; from friction at the roller surface prior to web tensioning; web material inhomogeneity. These residual stresses can take the form of non-uniform tension distribution across the width of the web and/or in-plane shear and lateral normal stresses. Ulsoy and Mote (1982) proposed general functional representations of the residual stresses without regard to the source. Mockensturm and Mote (1998), through the use of a nonlinear theory, calculated explicitly the residual membrane stresses that arise as the web is twisted due to roller mislaignment. In this article we deal with the effects of width-dependent tension that arises from non-uniform distribution of tension upstream or downstream of the span, that is $N_{xx} = N_{xx}(y)$. As pointed out in Mockensturm and Mote (1998), any distribution of residual stresses must satisfy strain compatibility relations. In particular, a tension distribution that is *linear* in the cross-span coordinate together with zero transverse shear stress is an admissible state of residual stress in the web.

The aerodynamic coupling of the web with surrounding air is also considered. Owing to the low mass density of paper webs, the added inertia of aeroelastic coupling can substantially lower the web frequencies and thus the critical speed (Niemi and Pramila (1987)). Niemi and Pramila (1987) demonstrated these effects for translating membranes using a finite element approach. In the present analysis we investigate the coupling of the translating, small bending stiff ness web model, with a surrounding incompressible potential flow. An aerodynamic potential $\phi(x, y, z, t)$ is defined throughout the fluid

domain. The pressure on the web $p(x,y,t)$ is the difference of aerodynamic pressure on the bottom and upper face of the web can be written as (Niemi and Pramila (1987))

$$p(x,y,t) = 2\rho_{air}\phi_{,t}(x,y,0^+) \tag{1}$$

Further, the inviscid flow assumption requires that the normal fluid velocity on the web equal the local component of transverse velocity at a point. The following non-dimensional quantities are introduced

$$u' = u/a, \quad x' = x/a, \quad y' = y/a, \quad z' = z/a$$
$$D = \frac{Eh^3}{12(1-\mu^2)}, \quad \varepsilon = \frac{D}{a^2 N_0}, \quad t' = \frac{1}{a}\sqrt{\frac{T}{\rho}}t, \quad N'_{xx} = \frac{N_{xx}}{N_0}, \quad N'_{yy} = \frac{N_{yy}}{N_0}, \quad N'_{xy} = \frac{N_{xy}}{N_0}$$
$$N_0 = \frac{1}{b}\int_{-b/2}^{b/2} N_{xx}(0,y)\,dy, \quad \Lambda = \frac{a\rho_{air}}{\rho}, \quad c' = \frac{c}{\sqrt{N_0/\rho}}, \quad \phi'(x',y',z',t) = \phi(x,y,z,t)\,a\sqrt{\frac{N_0}{\rho}} \tag{2}$$

where N_0 is the width averaged axial tension at the upstream boundary. *The primes denoting the dimensionless quantities are dropped in the subsequent analysis.* In the nondimensionalized variables, $\mathcal{A} = \{(x,y) \mid 0 < x < 1, -\kappa/2 < y < \kappa/2\}$ is the area of the web in the span. Appending the surrounding fluid pressure to the equations of motion of a flat, translating plate, (Ulsoy and Mote (1982)), the equations of motion and fluid continuity equations of the surrounding incompressible fluid can be written as:

$$\varepsilon\nabla^4 u + u_{,tt} + 2cu_{,xt} + c^2 u_{,xx} - \left[N_{xx}u_{,xx} + N_{xy}u_{,xy} + N_{yy}u_{,yy}\right] = 2\Lambda\phi_{,t}(x,y,0^+,t)$$
$$\text{on } \mathcal{A}$$
$$\nabla^2\phi = 0 \qquad \text{in } \mathcal{R}^3 \setminus \mathcal{A} \tag{3}$$

Recall that for the residual stress state discussed in this paper, $N_{xx}(y) = 1 + \beta y$, $N_{yy} = N_{xy} = 0$ where β is *a non-uniformity parameter* measuring the linear variation of tension across the width. The corresponding boundary conditions are:

$$u(0,y,t) = u(1,y,t) = 0, \quad u_{,xx}(0,y,t) = u_{,xx}(1,y,t) = 0 \quad \text{(simply supported at x = 0,1)}$$
$$u_{,yy}(x,-\kappa/2,t) + \mu u_{,xx}(x,-\kappa/2,t) = u_{,yy}(x,+\kappa/2,t) + \mu u_{,xx}(x,+\kappa/2,t) = 0$$
$$u_{,yyy}(x,-\kappa/2,t) + (2-\mu)u_{,yxx}(x,-\kappa/2,t) = u_{,yyy}(x,+\kappa/2,t) + (2-\mu)u_{,yxx}(x,+\kappa/2,t) = 0$$
$$\text{(free edges at } y = -\kappa/2, \kappa/2)$$

$$\phi_{,z}(x,y,0,t) = u_{,t} \quad \text{on } \mathcal{A} \quad \text{(velocity matching)}$$
$$\lim_{z\to\infty}\phi_{,z}(x,y,z,t) = 0 \quad \text{(farfield radiation condition)} \tag{4}$$
$$\phi_{,z}(x,y,0,t) = 0 \text{ outside } \mathcal{A} \text{ (baffled web)} \quad \text{or} \quad \phi(x,y,0,t) = 0 \text{ outside } \mathcal{A} \text{ (unbaffled web)}$$

The equations of motion (3) are discretized using Galerkin's method. The mass-normalized eigenfunctions, $\psi_{mn}(x,y)$ of a uniformly tensioned ($\beta = 0$), stationary web ($c = 0$) and without aerodynamic coupling ($\Lambda = 0$) are used as basis functions for the discretization of (3). The discretization is performed in the configuration space formulation of the gyroscopic eigenvalue problem. Accordingly

$$u(x,y,t) = \sum_{m=1}^{\infty}\sum_{n=1}^{\infty} q_{mn}(t)\psi_{mn}(x,y) \tag{5}$$

where the basis functions $\psi_{mn}(x,y)$ possess $m-1$ nodes along the X axis and $n-1$ nodes along the Y axis. Further the aerodynamic potential is also expanded as follows

$$\begin{aligned}\phi(x,y,z,t) &= \sum_{m=0}^{\infty}\sum_{n=0}^{\infty} A_{mn}(t)\varphi_{mn}(x,y,z) \\ \varphi_{mn}(x,y,z) &= \int_{\xi=-\infty}^{+\infty}\int_{\eta=-\infty}^{+\infty} B_{mn}(\xi,\eta)\, e^{i(\xi x+\eta y)}\, e^{-\sqrt{\xi^2+\eta^2}\, z}\, d\xi\, d\eta\end{aligned} \tag{6}$$

where A_{mn} and $\beta_{mn}(\xi,\eta)$ need to be computed so as to satisfy the boundary conditions at $z = 0$ of a *baffled* or *unbaffled* web. The expansion (6) not only satisfies the continuity equations for the fluid (3) but also the farfield radiation conditions (4). The unbaffled web assumption allows for exchange of fluid between the upper and lower half spaces thus modeling correctly the fluid motion bear the free edges of the web. This leads to a mixed boundary value problem at $z = 0$ consisting of a Neumann boundary condition on $\mathcal{A}$ and a Dirichlet boundary condition outside $\mathcal{A}$. The baffled web assumption precludes any exchange of the surrounding fluid between the upper and lower half spaces leading to slightly larger estimates of the added fluid inertia effect. However, this is computationally easier to solve because the boundary condition at $z = 0$ is a Neumann boundary condition. In this article we will outline a semi-analytical computation technique for the baffled web assumption.

Substitution of (6) and (5) into the boundary conditions (4) for a baffled web and the use of the inverse two-dimensional Fourier transform leads to

$$\begin{aligned}A_{mn}(t) &= -\dot{q}_{mn}(t) \\ B_{mn}(\xi,\eta) &= \frac{1}{\sqrt{\xi^2+\eta^2}} \int_{x=0}^{1}\int_{y=-\kappa/2}^{+\kappa/2} \psi_{mn}(x,y) e^{i(\xi x+\eta y)}\, dx\, dy = \frac{\psi^*_{mn}(\xi,\eta)}{\sqrt{\xi^2+\eta^2}}\end{aligned} \tag{7}$$

where $\psi^*_{mn}(\xi,\eta)$ is the two-dimensional Fourier transform of the basis function $\psi_{mn}(x,y)$ evaluated over $\mathcal{A}$.

For the Galerkin's method, we consider a N term expansion in equations (5) and (6) and require that the residual of the equations of motion converge to zero (Meirovitch (1997)). This is accomplished by substitution of equations (7), (6) and (5) into the web vibration equations (3) and through the use of inner products of the resulting equations

with any basis function $\psi_{ij}(x,y)$. This leads to the following discretized equations of motion

$$(\mathbf{I} + 2\Lambda\mathbf{M_{air}})\ddot{\mathbf{q}} + 2c\mathbf{G}\dot{\mathbf{q}} + (1-c^2)\mathbf{K_1}\mathbf{q} + \beta\mathbf{K_2}\mathbf{q} + \varepsilon\mathbf{K_3}\mathbf{q} = \mathbf{0} \tag{8}$$

where $\mathbf{I}$ is the $N \times N$ identity matrix, and

$$\begin{aligned}
(M_{air})_{ij;mn} &= \int_{\xi=-\infty}^{+\infty}\int_{\eta=-\infty}^{+\infty} \frac{\psi^*_{mn}(\xi,\eta)\,\overline{\psi}^*_{ij}(\xi,\eta)}{\sqrt{\xi^2+\eta^2}}\,d\xi\,d\eta \\
(G)_{ij;mn} &= \int_{x=0}^{1}\int_{y=-\kappa/2}^{+\kappa/2} \psi_{ij}(x,y)\,(\psi_{mn}(x,y))_{,x}\,dx\,dy \\
(K_1)_{ij;mn} &= -\int_{x=0}^{1}\int_{y=-\kappa/2}^{+\kappa/2} \psi_{ij}(x,y)\,(\psi_{mn}(x,y))_{,xx}\,dx\,dy \\
(K_2)_{ij;mn} &= -\int_{x=0}^{1}\int_{y=-\kappa/2}^{+\kappa/2} y\,\psi_{ij}(x,y)\,(\psi_{mn}(x,y))_{,xx}\,dx\,dy \\
(K_3)_{ij;mn} &= \int_{x=0}^{1}\int_{y=-\kappa/2}^{+\kappa/2} \nabla^4\psi_{mn}(x,y)\,\psi_{ij}(x,y)\,dx\,dy
\end{aligned} \tag{9}$$

$\mathbf{q}(t)$ is the vector of the generalized coordinates $q_{mn}(t)$ and $\mathbf{M_{air}}$ is the symmetric aerodynamic loading matrix (usually non-diagonal). The quantities with asterisks are Fourier transforms of the basis functions and the overbar denotes a complex conjugate. $\mathbf{G}$ is the skew-symmetric gyroscopic matrix, while $\mathbf{K_1}$ is the diagonal stiffness matrix contributed by the uniform component of the tension. The diagonal entries of $\mathbf{K_1}$ are the squares of the natural frequencies of an equivalently tensioned string i.e. $\pi^2, (2\pi)^2$ and so on. $\mathbf{K_2}$ is the symmetric stiffness matrix arising from non-uniformity of tension and $\mathbf{K_3}$ is the symmetric bending stiffness matrix.

Several key parameters appear in the discretized equations (8): $\Lambda, c, \beta,$ and ε. These represent respectively, the ratio of air density to web density, the non-dimensional transport speed, the non-uniform web tension parameter, and the web stiffness to applied tension ratio. Each plays a distinct role in the vibration and stability of the web and will be discussed in the following sections. Note that no aerodynamic or viscoelastic damping has been included in the model.

AN EXACT SOLUTION FOR FREQUENCY CLUSTERING

The self-adjoint eigenvalue problem for a stationary, uniformly tensioned, aerodynamically uncoupled web ($\Lambda = \beta = c = 0$) permits exact, separable solutions of the form

$$u(x,y,t) = \psi_{mn}(x,y)e^{\lambda t}; \quad \psi_{mn}(x,y) = \sin(m\pi x)Y_n(y) \tag{10}$$

Substitution of (10) into the equations of motion (3) and boundary conditions (4) with $\Lambda = \beta = c = 0$ leads the classical eigenvalue problem for a tensioned pinned-pinned, free-free plate. Letting $\lambda = i\omega$ and $Y_n(y) = e^{i\alpha y}$ in (11), the following relationship between ω and α emerges

$$\omega^2 - m^2\pi^2 = \varepsilon(\alpha^2 + m^2\pi^2)^2 \tag{11}$$

ω and α are determined through the substitution of (11) and (10) into the boundary conditions and requiring a nontrivial solution for the cross-span mode shape $Y_n(y)$. This requires the vanishing of the determinant of the coefficient matrix of the boundary conditions whose entries can be written either in terms of ω or α. The cross-span modes $Y_n(y)$ can be divided into symmetric and anti-symmetric modes corresponding to n being odd or even (shown for $m = 1$ in figure 2b). Clearly $\alpha = \alpha(m, \mu, \kappa)$, therefore from (11) for a given aspect ratio, Poisson's ratio and in-span mode number, the natural frequencies of all the corresponding cross-span modes are controlled through the parameter ε. As $\varepsilon \to 0$, the natural frequencies of all the cross-span modes of the web can be brought arbitrarily close to $m\pi$, the natural frequency of an equivalently taut string. The resulting occurrence of several closely spaced frequencies is referred to as frequency clustering (Tzou *et. al.* (1998)). Further from (11) each frequency cluster is of $O(\varepsilon)$.

Dimensionless natural frequencies of first three symmetric and anti-symmetric cross-span modes (six total) corresponding to $m = 1,2,3$ as a function of $\log_{10}\varepsilon$ are calculated for a web with $\mu = 0.3$ and $\kappa = 0.4435$ in figure 2a. At $\varepsilon = 10^{-6}$, at least six cross-span modes are tightly clustered within 1 % of the corresponding frequencies of a taut string. *Frequency clustering in very flexible webs is manifest in a multitude of cross-span modes with nearly identical frequencies.* For a fixed ε, the greater the m, the tighter the frequencies cluster. For each m, the lowest symmetric mode (bending) and the lowest anti-symmetric mode (torsion) have nearly identical frequencies for $\varepsilon < 10^{-3}$ indicating that *frequency clustering in stiffer webs takes the form of two nearly repeated frequencies of the first bending and first torsional mode.*

Frequency clustering has several implications for the modal analysis, stability, and nonlinear vibrations of thin webs:

1. Forced vibration at the natural frequency of one mode in a cluster leads to all modes in the cluster participating in the response. This can render indistinguishable several cross-span modes during experimental modal analysis of web vibrations.
2. *The participation of several cross-span modes in the response leads to overall motions of the web that tend to be localized near the free edges.* Consider the equal participation of only the first three symmetric cross-span modes in the forced response (figure 2b). The three modes may oppose each other in the middle of the span but reinforce each other at the free edges. Similarly consider the participation of the first three symmetric and anti-symmetric modes (figure 2b) in the response. Clearly their superposition leads to small vibration in the middle of the span and one edge, and large vibration near the other free edge. The overall shape of vibration near a natural

frequency then depends on the location of the forcing and its frequency with respect to the frequency cluster.

3. Modes in a frequency cluster are in a state of one-to-one internal resonance. Large amplitude nonlinear vibration of any one mode will couple nonlinearly to every other mode in the cluster. Smaller the ε, the larger the number of modes participating in the response.
4. Any instability of the thin web will occur simultaneously for all modes in a cluster leading to unstable mode shapes not resembling any individual mode but rather being a superposition of several distinct modes all with the same m but different number of nodes in the Y direction.

EFFECTS OF WEB SPEED, NON-UNIFORM TENSION AND AERODYNAMIC LOADING

The integrals that constitute the elements of the matrices (9) are evaluated numerically using MAPLE V and MATLAB (except the aeroelastic loading matrices) . The eigenvalue problem of the discretized equations (8) is numerically solved to yield the approximate natural frequencies of the web. Numerical convergence studies are carried out to ensure that a sufficient number of basis functions are included in the approximation (equations (5) and (6)). Sixty basis functions (eigenfunctions of the stationary web) are assembled representing $m = 1..6$ in-span modes and five symmetric and five anti-symmetric cross-span modes for each m.

Subsets of these functions are appropriately chosen to approximate the desired eigenfunctions. For instance, to calculate the lowest anti-symmetric mode frequencies $(n = 2)$ for $m = 1,2,3$ when $\beta = 0$, a six-mode approximation consisting of the lowest anti-symmetric modes for $m = 1..6$ converges to the second decimal place, for moderate transport speeds. Because the eigenfunctions of the continuous system are complex with nonconstant phase, the use of stationary web eigenfunctions provides slower convergence than through the use of complex eigenfunctions especially at subcritical speeds. However the eigenfunctions of a translating web are not known exactly. For this reason stationary web eigenfunctions were used as a basis for the Galerkin's discretization. As another example, when $\beta \neq 0$ and $c = 0$, the resulting eigenfunctions are no longer purely symmetric or anti-symmetric in the cross-span. Hence both symmetric and anti-symmetric basis functions are to be included in the approximation when $\beta \neq 0$.

Effects of transport speed

The approximate natural frequencies of the first three symmetric and anti-symmetric modes ($n = 1..6$) corresponding to $m = 1,2,3$ are computed as a function of transport speed for a paper web with $\varepsilon = 10^{-5}$, $\mu = 0.3$, and $\kappa = 0.4435$ are shown in figure 3. Frequency clusters corresponding to different in-span mode numbers remain distinct at low to moderate transport velocities (figure 3). However, with increasing transport speeds the overlap between frequency clusters increases. Indeed near critical speed, several modes in a cluster will buckle (wrinkle) simultaneously leading to spatially complex buckled mode shapes. This complicated behavior of the linear web model underscores the importance of nonlinear web models especially near critical speed.

Effects of non-uniform tension

The lowest two natural frequencies of a stationary web (the first symmetric and anti-symmetric mode) are plotted as a function of the nonunifomity parameter β for $\varepsilon = 10^{-5}$, $\mu = 0.3$, and $\kappa = 0.4435$. Five cross-span symmetric and five anti-symmetric modes were used in the approximation. These two modes possess nearly identical frequencies form a uniform web. It is seen that the symmetric mode frequency reduces and that of the anti-symmetric mode increases. This is also seen in roll tensioning of band saws (Ulsoy and Mote (1982)). Eventually the symmetric mode will buckle. Interestingly, when $\beta \neq 0$ the cross span modes can no longer be divided into purely symmetric and anti-symmetric modes i.e. they are coupled. The coupling occurs only between symmetric and anti-symmetric modes belonging to the same frequency cluster (same m). Therefore the net effect of non-uniform tension is to split apart frequency clusters by reducing the frequency of the symmetric modes and increasing those of the anti-symmetric ones.

Effects of aerodynamic coupling

The general semi-analytical procedure for computing the aeroelastic coupling effect of a baffled web was described earlier. However, the computational results are not presented in this article. We note that the aerodynamic coupling also couples together otherwise distinct modes of the web thereby greatly complicating the analysis. The integrals in the aerodynamic loading matrix $\mathbf{M}_{\mathbf{air}}$ involve non-removable singularities and are to be computed using special singularity handling quadratures such as the IMSL subroutines. In general, though, the added mass coefficient on the lowest symmetric mode is usually the greatest since it tends to displace the greatest volume.

EXPERIMENTAL RESULTS

Experiment description

Experiments were performed on a stationary paper web stretched over two smooth rollers (figure 4 a). For the paper $\rho = 88.1 gm/m^2$, $a = 0.712m$, $b = 0.316m$, with $\kappa = 0.4435$. It may be noted that since paper is a porous material, it loses some weight in the form of moisture over time. The web is wrapped around and taped uniformly to one roller, while the other end is passed over a roller and weighted down outside the span with a smooth steel rod. The smooth rollers and the distributed weight ensure an even cross-span tension distribution, and minimal residual shear stress in the web. An initial weight of $3.5kg$ is applied leading to $N_0 = 108.65 N/m$ tension per unit width of the paper. This tension lies in a fairly typical range for paper web handling systems. The rollers are aligned in parallel using an optical alignment system. Another frame carries the loudspeaker used to excite the web.

Laser triangulation sensors were found appropriate for non-contact measurement of paper web vibration (from Weinglorz Inc.). These sensors measure directly the motion of a laser spot on the surface as the surface vibrates. The web is divided into a 7×9 grid and the sensors are used to measure the vibration of the web at 63 points on the web. The web is excited acoustically by a loudspeaker (woofer), which is carried by a second frame (figure 4 a). The gain of the speaker is fairly constant in the 10-100 Hz range. A HP4194A

gain-phase analyzer samples the data from the sensors and drives an output current to the amplifier for the speaker. This allows for very slow sweep rates and accurate frequency resolution of peaks. Accurate measurement of the frequency response of the paper web in the 10-100 Hz range takes more than two hours.

To measure the frequency response function of the web, the speaker is placed near a free edge and away from the mid-span of the web (figure 4 b). Since all the cross-span modes have non-zero displacement at the free edges, this arrangement ensures that most cross-span modes will be excited. The speaker is centered at point (6,2) (figure 4 b). The response of the web is measured at the other marked points of the web. The gain and phase of the web at different points is measured with respect to the driving current of the speaker. The frequency response function of the web is then deduced by dividing the total frequency response function by the frequency response function of the speaker.

To determine the resonant shapes of the web, the speaker is driven at a chosen peak of the web frequency response function. The web is allowed to reach a steady state, and the response is measured pointwise at 63 points on the web. Both the gain and phase information are recorded. The measured modeshapes are then plotted using the spline interpolation technique in MATLAB.

Results and discussion

A typical plot of the gain of the web transfer function measured at point (6,2) is shown in figure 5. The lowest frequency of the web is at 11.475 Hz. Several other peaks are observed below 100 Hz. The damping of the modes increases with increasing frequency. The prominent modes can be grouped approximately into three categories corresponding to $m = 1,2,3$ clusters, respectively (figure 5). The modeshapes corresponding to the peaks at 11.475 Hz, and 15.035 Hz in the $m = 1$ cluster, 31.58 Hz in the $m = 2$ cluster and 61.86 Hz in the $m = 3$ cluster are measured in detail. The gain of the response measured at the above four forcing frequencies is plotted in figure 6.

At each resonant forcing, the phase of the response varied from being nearly in-phase with the forcing near the speaker location and lagging behind the forcing at other web locations. The phase distribution is not plotted because of large errors in estimating the phase lag near nodal lines. However, away from the nodal lines the phase distribution was well behaved for the resonant mode shapes at 11.475 Hz and 15.035 Hz. The shapes at 11.475 Hz and 15.035 Hz were characterized by slightly non-constant phase distributions with slightly greater phase lag away from the speaker. Additionally the shape at 15.035 showed a clear switching of phase angle across the nodal line at the X axis. The resonant mode shapes at 31.58Hz and 61.86 Hz displayed a greater non-constancy of phase.

The natural frequencies of an equivalently taut string for this experimental web can be calculated to be $24.66 \times m$ Hz where m is the in-span mode number. In the absence of aerodynamic coupling the web frequencies should theoretically cluster about these string frequencies. However the aerodynamic coupling reduces the frequency of the fundamental mode (11.475 Hz) by nearly 54 %. As expected, the fundamental mode frequency is the most affected by aerodynamic coupling.

The cross-span resonant shapes do not resemble any individual cross-span mode (figure 3 a). For example the resonant shape at 11.475 Hz can be thought of as a combination of the $n = 1,3$ cross-span mode shapes (see figure 3 a). The resonant shape at 15.035 Hz can be regarded as a combination of the $n = 2,4$ cross-span mode shapes. The cross-span resonant shapes for the higher frequency clusters ($m = 2,3$) are quite complex indicating a greater degree of frequency clustering as predicted by the analysis. Interestingly, for excitaiton frequencies at 31.58 Hz and 61.86 Hz, it is hard to locate any nodal points even in the X direction. The resonant shapes at 31.58 Hz and 61.86 Hz clearly correspond to $m = 2,3$ respectively, however the presence of contamination from the $m = 1$ cluster is evident.

The participation of the fundamental mode in the resonant response of higher modes is often found in the modal analysis of damped continuous systems (Soedel (1993)). The presence of strong damping may also be indicated by the non-uniformity in phase distribution. Damping mechanisms for paper webs can arise from viscoelasticity or viscous effects of the surrounding fluid, neither of which were modeled in the present analysis. Clearly the inclusion and investigation of damping mechanisms in paper webs and the use of nonlinear web models is likely to yield more accurate predictions of the resonant shapes.

CONCLUSIONS

1. For stationary, uniformly tensioned, aerodynamically decoupled webs, the frequencies of cross-span modes cluster about the corresponding frequency of an equivalently tensioned string.
2. Frequency clustering leads to web vibration localization near the free edges of the web and can seriously impede modal analyses and complicate the nonlinear dynamic analyses of the web.
3. Non-uniform tension splits each frequency cluster into two, corresponding to symmetric and anti-symmetric cross-span modes. The resulting mode shapes do not remain purely symmetric or anti-symmetric across the span. Large non-uniformity of applied tension can lead to buckling (wrinkling) of some modes.
4. Frequency clusters remain distinct at low to moderate transport velocity. However near critical speed, the clusters merge resulting in the web buckling in several mode clusters.
5. Aerodynamic coupling can reduce significantly the web frequencies and spread apart the frequency clusters.
6. Experiments performed on stationary webs confirm the occurrence of frequency clusters. The measured mode shapes for the lowest frequency cluster show superposition of more than one cross-span mode in the cluster. However for higher frequency clusters, the measured mode shapes show many other influences including contamination form the fundamental mode. The non-constancy of phase in the resonant mode shapes could indicate the presence of strong damping in the system.

REFERENCES

1. Steigmann, D. J., Pipkin, A.C., "Equilibrium of Elastic Nets," Philosophical Transactions of the Royal Society of London A, Vol. 335, 1991, 419-454.

2. Lin, C. C., Mote Jr., C. D., "The Wrinkling of Thin, Flat, Rectangular Webs," ASME Journal of Applied Mechanics, Vol. 63, No. 3, 1996, 774-779.
3. Mockensturm, E. M., Mote, Jr., C. D., "Steady Motions of Translating, Twisted Webs," International Journal of Nonlinear Mechanics, Vol. 34, No. 2, 1999, pp. 247-257.
4. Lin, C. C., Mote Jr., C. D., "Equilibrium Displacement and Stress Distribution in a Two-dimensional, Axially Moving Web under Transverse Loading," ASME Journal of Applied Mechanics, Vol. 62, No. 3, 1995, 772-779.
5. Mockensturm, E. M., "On the Finite Twisting of Translating Plates," Ph. D. Thesis, University of California, Berkeley, 1998.
6. Wang, M. P., Steigmann, D. J.,"Small Oscillations of Finitely Deformed Elastic Networks," Journal of Sound and Vibration, Vol. 202, No. 5, 1997, 619-631.
7. Ulsoy, A. G., Mote Jr., C. D., "Vibrations of Wide Band Saw Blades," ASME Journal of Engineering for Industry, Vol. 104, 1982, 71-78.
8. Turnbull, P.F., Perkins, N.C., Schulz, W. W., "Contact-induced Nonlinearity in Oscillating Belts and Webs," Journal of Vibration and Control, Vol. 1, 1995, 459-479.
9. Niemi, J., Pramila, A., "FEM-analysis of Transverse Vibrations of an Axially Moving Membrane Immersed in Ideal Fluid," International Journal for Numerical Methods in Engineering, Vol. 24, 1987, 2301-2313.
10. Meirovitch, L., Principles and Techniques of Vibrations, Prentice-Hall, 1997.
11. Tzou, K. I., Wickert, J. A., Akay, A., "Frequency Clusters in the Spectrum of Annular Cylinders," ASME Journal of Applied Mechanics, Vol. 65, No. 4, 1998, 797-803.
12. Soedel, W., Vibrations of Plates and Shells, 2nd ed., Marcel-Dekker, 1993.

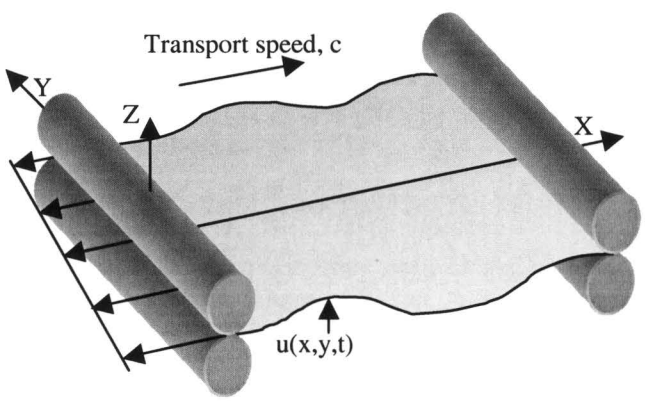

Figure 1. A schematic of the translating web system with non-uniform tensioning and aerodynamic coupling with incompressible potential flow.

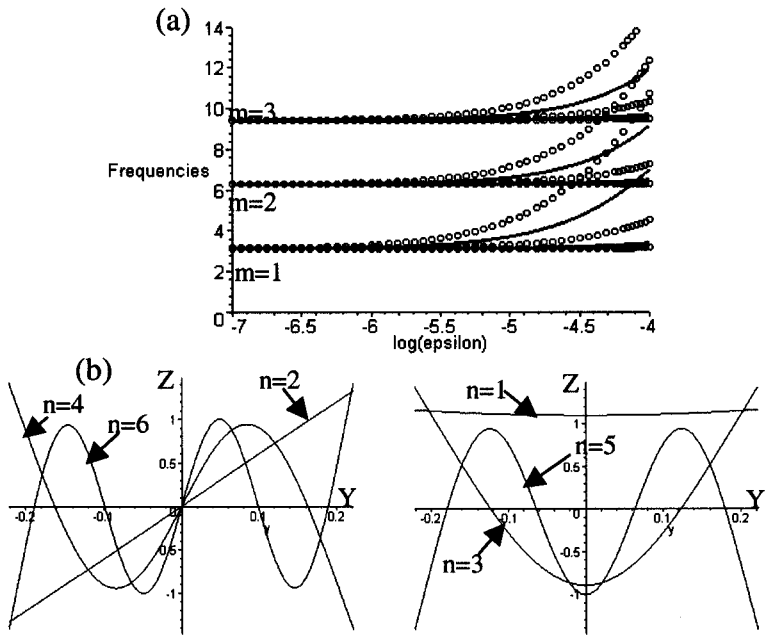

Figure 2. (a) Frequency clustering of a stationary, uniformly tensioned, aerodynamically uncoupled web. (o anti-symmetric cross-span modes, - symmetric cross-span modes). (b) The anti-symmetric and symmetric cross-span mode shape

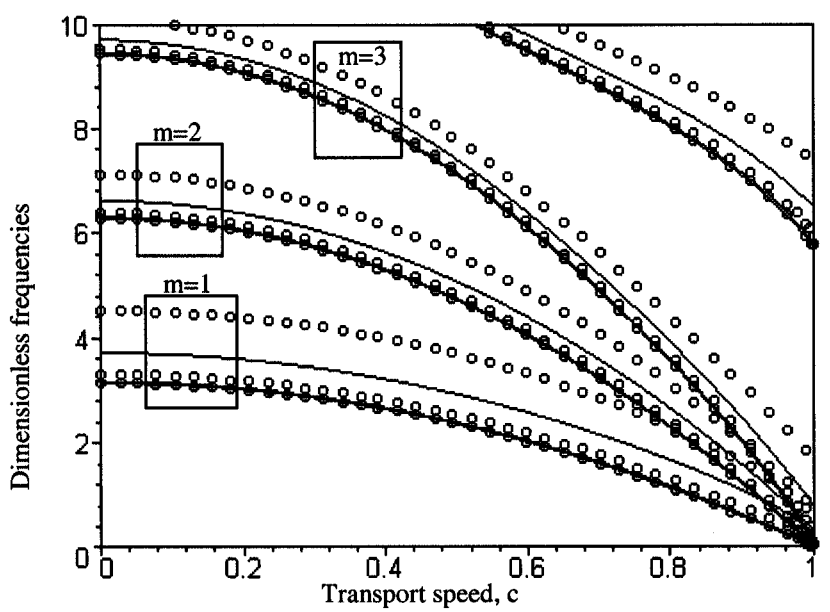

Figure 3. Variation of web natural frequencies (o anti-symmetric, - symmetric) with transport speed, c.

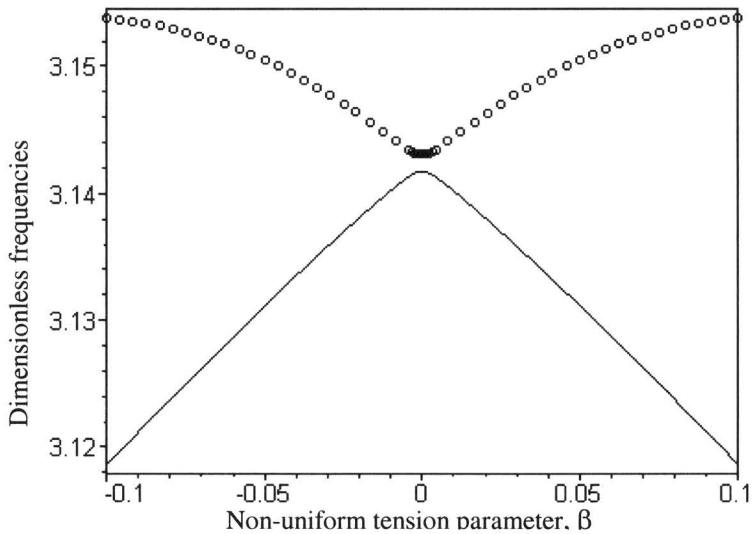

Figure 4. Variation of the first symmetric and anti-symmetric mode frequencies with nonuniform tensioning (o anti-symmetric, - symmetric).

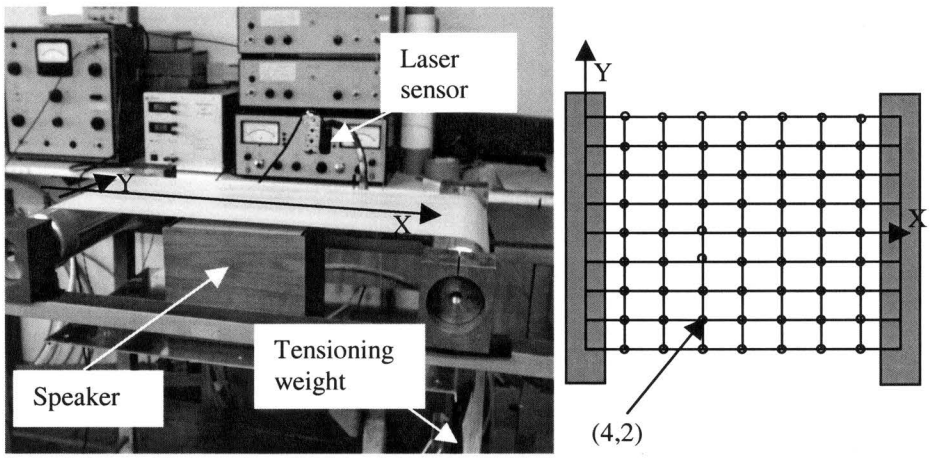

Figure 5. (a) Experimental configuration, and (b) measurement grid on the web (small circles denote the measurement points).

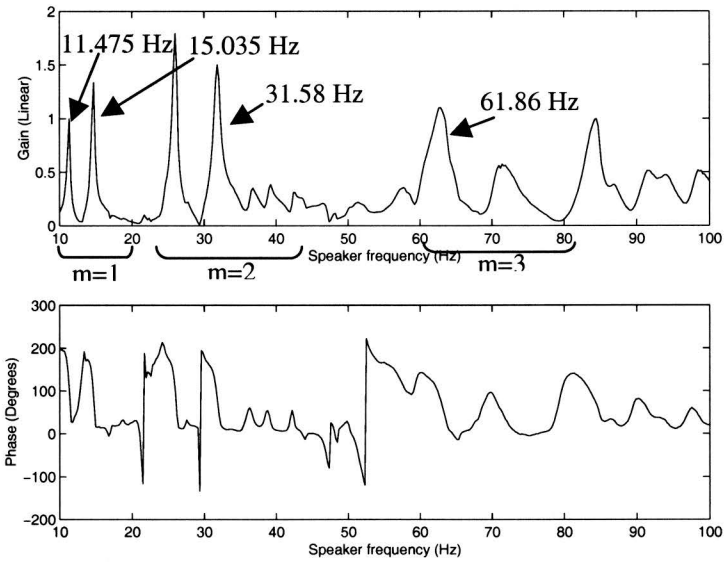

Figure 6. Gain and phase of the frequency response function of the web measured during a slow sweep of excitation frequency. Measurement point is collocated with the speaker at point (6,2) on the measurement grid.

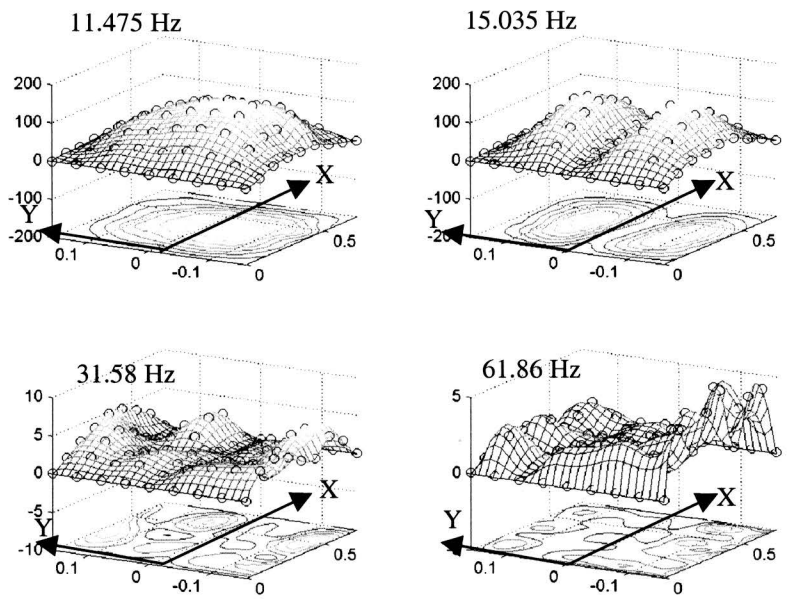

Figure 7. Gain of the web frequency response function at the excitation frequencies 11.475 Hz, 15.035 Hz, 31.58 Hz, 61.86 Hz measured at different points on the web. Note that the phase angle switches across nodal lines.

A. Raman[1], K. Wolf[2], and P. Hagedorn[2] – [1]Purdue University, USA, and [2]Technical University Darmstadt, Germany

Name & Affiliation	**Question**
D. Pfeiffer – JDP Innovations	I would like to suggest that the authors consider another form of air coupling, particularly on web edges, and that is vortices generated by the windage crown, a traveling web coming up against a stationary roll, so there would be shedding vortices on left and right sides of the machinery and vortices are very powerful. If you've seen them being shed from tractor-trailer trucks going down the highway, you see one on each side of the truck, and they can tear the canvas covers off. Coupling of vortices with the flopping edge of the web could be a reason for web tears on the edge of the web.
Name & Affiliation	**Answer** (fielded by P. Moretti who represented the authors)
P. Moretti – OSU	I take your point, I am a bicyclist, so I'm familiar with the phenomenon of passing trucks. The authors have mentioned vortex shedding but have not investigated excitation mechanisms. You'll find that Y. B. Chang of OSU has worked on excitation and you might talk to him. At this point, this paper only includes aerodynamic inertia, and not the excitation effects of air. The authors postulated two potential flow fields. For one of them, the air can move around the edges; on the other one, there is a baffle. They started with the latter calculation, because it has classic boundary layer conditions. Aerodynamic inertia loading shows how important the results are. I think your point is well taken: because of the air mass/web mass ratio, air structure interaction effects are absolutely vital to excitation, just as they are to inertia frequency, as the authors demonstrate. There are many aspects to fluid structure interaction and I expect us to be busy with these problems for a long time.
Name & Affiliation	**Comment**
G. Homan – Westvaco	I'd like to compliment you on a fine job. I'd like to springboard off of what David had said: I think you did a superb job. I have no idea how long you had a chance to prepare, but it was nicely done.

Name & Affiliation	Reply
P. Moretti – OSU	Well, thank you very much. I'm very enthusiastic about this paper. I think it's a valuable paper, and I'm glad I got that across to you.
Name & Affiliation	**Question**
R. Swanson – 3M	The paper shows the mode shapes of the vibrations. What is your comment on when will it vibrate? How fast can we run before it does vibrate? How high can the air velocities in our ovens be before the onset of vibration?
Name & Affiliation	**Answer**
P. Moretti – OSU	Well, this paper focuses on the sensitivity of the web to vibration by identifying the natural frequencies and modes. When you know the frequency of the excitation source, like an unbalanced roll, a defect in tension control system, or a vortex shedding excitation, this tells you how to avoid problems. What Professor Y. B. Chang and I have done is at the other side of the physical problem, looking at the excitation due to air motion. What we need to do is bring the two together combining the sophisticated structural dynamics of this paper with aeroelastic excitation. This paper has motivated me to look at that again, but I can't tell you today where it will lead.

Discussion of Sessions 2 and 3 **Dr. Karl Reid** – OSU

Name & Affiliation	**Question**
S. Lange – Procter & Gamble	This question is for Jim Dobbs. In your paper, you showed that in all cases where the incoming web tension was lowest, it gave the highest tension ratio, which is sort of counter intuitive. Do you have any theories on why that was?
Name & Affiliation	**Answer**
J. Dobbs – 3M	My theory is that at lower tensions, the web may be pulled into the grooves, and there is a mechanical locking that results in the higher tension ratio.
Name & Affiliation	**Comment**
S. Lange – Procter & Gamble	If you had tested different rollers you might be able to see that effect.
Name & Affiliation	**Comment**
D. Jones – Emral, Ltd.	If you remember my talk this morning, I had an analytical model for what should replace the belt equation when you have air entrainment, with an extra air pressure under the web. I think if you made Pa negative that may well be appropriate to the vacuum pull roll case. I can see it may work when you have a mesh, or sintered metal type of roll, but it may be a little bit more difficult to apply in Jim's case where he only has small regions where the web is in contact with the surface.
Name & Affiliation	**Answer**
J. Dobbs – 3M	That is certainly something I'll be looking into.
Name & Affiliation	**Comment**
R. Lucas – GL&V	Relative to this observation on increased tension ratios at low tension levels, and your explanation as to possible deformation of the web into the groove: if you were to discuss grooves that might be intended for traction on surface winders, it is not uncommon for us to see increased traction that we have rationalized can only be developed if the paper is deforming into the groove. So there seems to be some other supporting evidence that your theory is correct.

Name & Affiliation	Question
T. Walker – TJWA	This question is for Young Chang. Did your work determine the nip load required to keep air bubbles out of laminates?
Name & Affiliation	**Answer**
J. Shelton – OSU	Young Chang demonstrated that the force does not have to be very large to keep the ballooning from occurring. An air knife instead of a roller might keep it from occurring, but you cannot use an air knife on a winding roll if the eccentricity is very great.
Name & Affiliation	**Question**
A. Henig – Aprion Digital, Ltd.	This is a general question about dancers. We are trying now to use in a torque motor at the base of the dancer, to enable a very quick response to start and stop of a printing machine. I want to know if there is any work done on such dancers and if somebody has any opinions on whether this is better than a piston and cylinder and those kinds of actuators.
Name & Affiliation	**Answer**
D. Carlson – 3M	That is the approach Pagilla's taking to an active dancer, where instead of passively allowing the dancer to move or be pulled where it is, you're going to drive it and take up that web, take up that slack. If you run it passively, the same equations apply except instead of the dancer cylinder you substitute the equipment for the torque motor. The difference is either applying a constant force to load the cylinder, then it is passive, or you're regulating the position of using a torque on the lever arm. So it's either a passive case or the active case. If it is the active case then Pagilla's analysis would apply
Name & Affiliation	**Question**
B. Walton – Eastman Kodak	I'd just like to speculate about using torque from a motor to apply torque to a float arm. You never get enough torque without some gearing. The gearing in turn would introduce too much hysteresis and way too much inertia, so I don't think that would be practical.
Name & Affiliation	**Answer**
D. Carlson – 3M	There are companies that manufacture low rpm, high torque motors, very expensive, very large diameter, and generally not economically feasible for the improved performance.
Name & Affiliation	**Question**
K. Reid – OSU	Is there a science base for understanding grooved rollers in the context of traction?

Name & Affiliation	Answer
K. Good – OSU	Keith Ducotey published some results of a three dimensional traction model in the July 2000 Journal of Tribology. The model incorporates plate bending as well as membrane effects for the web coupled with a Reynolds solution for the entrained air beneath the web. The model exhibits the web undulation that occurs at the exit as well as the anticlastic effects that exist at the edges that cause the web to bend down and approach the roller surface. The model also incorporates the impact of grooves on air film thickness and on traction. The results of Keith's model very much remind me of the camera pictures that Jim Dobbs was showing earlier today with the air entrapped over the diamond patterns. Keith's model showed that much of the traction was due to the web touching the edges of the holes or grooves in the rollers and that air became trapped in the land areas. The model also showed that the web does pull down into the grooves as Jim Dobbs was describing earlier.
Name & Affiliation	**Comment**
D. Jones – Emral Ltd.	I was not aware of any other published work before I put my review together. Keith Ducotey's results are recent in this area. It appears he has included the elements to model the situation. You do need to include some resistance to the bending of the web. My work has treated the web as a perfectly flat spool membrane. The only way you can avoid that is if the web stays more or less conforms to a cylindrical shape, which I believe the Hashimoto papers have treated it in the past.
Name & Affiliation	**Comment**
J. Dobbs – 3M	I reviewed what Hashimoto presented at the 1999 IWEB. It incorporated an area correction factor for the cross sectional area of the grooves. I have as well done this in the past for rough estimations of how much to groove or knurl a roll.
Name & Affiliation	**Comment**
B. Feiertag – OSU	There is a practical side of this that I see a lot. People often design wide grooves that are circumferential or in many cases with very shallow helical angles. The web tends to pull down into the grooves which is a problem for thin webs. A relatively high helical angle combined with a relatively narrow groove is helpful. Keith Ducotey's work proved that just the existence of the grooves produces a lot of edge effects, which helps you get a hold on the web. I believe using fairly narrow 30 degree helical grooves which are efficiently cut is the thing to do to get rid of the air. This configuration does not produce a tendency of the web to drop down into the grooves.

Name & Affiliation	Comment
K. Good – OSU	Many of you have seen micro-grooved rollers where the grooves look almost like scratches on the roll surface. Keith Ducotey's model showed that micro grooving is effective in venting the air and that most grooves are cut way to wide and deep. In the present discussion we are talking about the webs pulling down into the grooves and that after this occurs the air is trapped in the land areas. Micro-grooves prevent this and the web damage aspects that Bruce is describing. The disadvantage of micro grooves is that they can be easily fouled by some webs. So there are advantages to micro-grooved rollers if your web won't foul the micro-grooves.
Name & Affiliation	**Answer**
D. Roisum – Finishing Technologies	These comments on roller grooving are quite fine, but there's one other thing you've got to keep in mind that's a big fallacy about grooving. There is no flow through the channel of the groove, so you do not need grooving at all. All you need is a place to park the air. So simple roughness of any kind will do the job, whether it be particles on the surface or shot peening or whatever.
Name & Affiliation	**Answer**
R. Lucas – GL&V	I disagree with you, Dave, a lot of air gets pumped through those grooves, at least the grooves we've been accustomed to using. Some of Dave Daley's work in the 1960's demonstrated that as he made the grooves deeper and deeper, the traction that he gained at high speed was higher than what it was at low speed. There was a definite Bernouli phenomenon that was increasing traction at high speed. We later observed that pieces of tape that were put over the groove ended up getting paper dust on the underside (sticky side) of the tape, strongly suggesting that there was air flow going through the grooves. When a web approaches a roll, you have a stagnation pressure on one side and a film splitting mechanism on the discharge side, which creates a forcing function to encourage air to go through these grooves. Thus I believe that you will find that you have a lot of air going through. I will submit that if you have a very small groove that is wrapping a large diameter drum, you basically have a curved tube with obvious limitations in air flow, so in those cases you see demonstrations where the air groove will become saturated. At that point the web will develop enough stagnation pressure to pick the wound roll up off of the rotating roll and everything fits together without any problem. It all makes sense to me anyway.
Name & Affiliation	**Comment**
J. Shelton – OSU	I would like to return to a topic from the Monday discussion. A bit of a surprise was the discussion of

	corrugations, when the subject was air entrainment because you can have corrugations without air entrainment. I presented a paper at IWEB 95 concerned with troughs and corrugations. The corrugations in wound rolls are the buckling of a thin web which is a pressurized cylindrical shell, the pressure resulting from web tension. The wave length is readily predictable. If you wind a roll that has corrugations and then wind one at twice the diameter, the wave length of the corrugations will be 1.4 times greater. That has been verified time and time again, from my wife's plastic wrap to very large rolls of thick web materials. Of course corrugations can be a problem, because they can result in permanent set. They are very difficult to prevent and I do not think we have time to speculate on how you can prevent it. But knowing where it came from is helpful. When you see a set of permanent corrugations, you can determine whether it happened when it was in roll A or roll B. After it was rewound, there is only one place in the web that had the same diameter in the last roll as it did in the parent roll. So you can tell where the permanent set occurred. But you see corrugations in metalized webs that are wound in a vacuum, so it is not the result of air entrainment. The corrugations affect the entrainment, and that has not been studied. You see corrugations on cylinder rollers and I cannot believe that the Knox- Sweeney equation would predict even the average value of the air entrainment. So the corrugations result because of lateral compression. Lateral compression may come from many sources. There is nothing except using effective spreading devices, which are rare, and tenters that pull the web out laterally. And everything appears to make the web gather. Don Sexton was complaining that we had not said much about viscoelastic memory but he knows about this problem and the effect of viscoelastic memory on corrugations. A web that has just been made or oriented, and has traveled down the line, is tensioned all the time in the machine direction but has nothing in the spans pulling it out laterally. So it gets wound up. The web will remember something from when it was relaxed and it attempts to shrink lengthwise. Art Fisher at Mobil several years ago had two precisely spaced pins on a beam compass. He pricked the roll with the beam as quickly as he could after it was wound, and then measured the distance between the two pin pricks versus time, and they moved wider apart. The web on the roll was expanding in width as it was shrinking in length. This is a recipe for buckling of a cylindrical shell. The result is that across most of the width of the roll you see corrugations because it expanded in width if it is a web that has just been oriented like I've just been describing.

Name & Affiliation	Comment
D. Pfeiffer – JDP Innovations	We saw corrugations form in the humid atmosphere in Philadelphia when we would open a roll of dry bond paper to the humid air there. You would immediately, before your eyes, see corrugation rings form around the roll as the humidity crept into the paper. We measured the expansion and increased 4% in width for a 25% increase in humidity.
Name & Affiliation	**Comment**
A. Thill – Exxon Mobil	John Shelton mentioned corrugations in metalized film. The corrugation appears only when you have opened the vacuum chamber. If you look at the winding roll during metalization, there are no corrugations on it. As you let the air into the vacuum chamber, you see the corrugation appear while you observe it. The roll is changing in diameter due to the pressure of the air that enters from the outside and the roll collapses. Now the roll circumference has reduced, so the loss of strain that you had in the MD is compensated by widening in the TD. Now the web cannot expand in the TD because the edges are blocked. It must corrugate.
Name & Affiliation	**Question**
K. Good – OSU	Is the wound roll of web that was just metalized hot? Do we have a hot wound roll, we open the chamber and introduce cool air?
Name & Affiliation	**Answer**
A. Thill – Exxon Mobil	No, the web is already cold when it is wound. The roll is probably wound at 30 degrees Celsius.
Name & Affiliation	**Comment**
J. Shelton – OSU	I certainly acknowledge Andre as the expert in this subject. I have witnessed wound metalized rolls out of the oven that were corrugated, and I haven't heard that explanation. I'm certainly not going to argue with Andre because I have not worked closely with a metalizer. I assumed that the corrugations occurred while it was in the vacuum. But still Andre described the source of a TD compression which caused the buckling of a cylindrical shell.
Name & Affiliation	**Answer**
A. Thill – Exxon Mobil	When you wind the roll, by the fact that you have a higher diameter in the center, this pulls the web toward the center, and rather than having a spreading effect on the winder, it has a shrinking effect on the winder. If we could calculate what kind of pressure profile we need on the contact roll to make the wound roll become more concave it would induce a positive TD strain that would compensate for the contraction afterwards.

Name & Affiliation	Question
K. Reid – OSU	In the last several papers today, authors mentioned work yet to be done.. There's obviously a lot of thinking that has occurred on what should come next. Who would like to venture out with a comment on—where's the biggest gap in the areas we talked about? Winding yesterday and other topics today. Where is the biggest gap? Where do we need to focus our efforts the most?
Name & Affiliation	**Answer**
R. Swanson – 3M	Keith Good alluded to it yesterday, and I'll talk about it tomorrow. I think there's a big gap in winding between our well developed stress models and the failure modes in winding.
Name & Affiliation	**Answer**
K. Cole – Eastman Kodak	I agree with Ron that failure predictions are a big need. I believe one of the other things that is needed is better models to predict some of these defects, we need a better 3-dimentional or better 2-dimensional models. A lot of these defects like corrugations and so forth require fully 3-dimensions. What we have right now in 3-dimentional models is segmented 2-dimensional models. I think if we had a better 3-dimensional model we could probably get at some of those defects.
Name & Affiliation	**Answer**
D. Roisum – Finishing Technologies	I think our biggest gap or challenge is technology transfer. I think a lot of us are in the research area, and we do not do the best job in selling our wares and teaching other people what we already know. So the biggest gap is not in what we do not know but what we do know and doesn't get translated down into practice.
Name & Affiliation	**Comment**
K. Reid – OSU	With that let me thank you for a very rich discussion this afternoon.